nature ecology & evolution

ARTICLES

https://doi.org/10.1038/s41559-018-0651-y

Evolutionary potential of transcription factors for gene regulatory rewiring

Claudia Igler[1,3], Mato Lagator[1,3], Gašper Tkačik[1], Jonathan P. Bollback[1,2] and Călin C. Guet[1*]

Gene regulatory networks evolve through rewiring of individual components—that is, through changes in regulatory connections. However, the mechanistic basis of regulatory rewiring is poorly understood. Using a canonical gene regulatory system, we quantify the properties of transcription factors that determine the evolutionary potential for rewiring of regulatory connections: robustness, tunability and evolvability. *In vivo* repression measurements of two repressors at mutated operator sites reveal their contrasting evolutionary potential: while robustness and evolvability were positively correlated, both were in trade-off with tunability. Epistatic interactions between adjacent operators alleviated this trade-off. A thermodynamic model explains how the differences in robustness, tunability and evolvability arise from biophysical characteristics of repressor–DNA binding. The model also uncovers that the energy matrix, which describes how mutations affect repressor–DNA binding, encodes crucial information about the evolutionary potential of a repressor. The biophysical determinants of evolutionary potential for regulatory rewiring constitute a mechanistic framework for understanding network evolution.

From the seminal discovery of repression and activation as the basic mechanisms of gene regulation[1,2], a fundamental picture has emerged, where individual regulatory components—promoters and transcription factors (TFs)—are interconnected into gene regulatory networks (GRNs): global structures that determine cellular gene expression patterns. However, a mechanistic understanding of how GRNs evolve is still lacking. GRN evolution can be studied at two opposing levels of organization: (i) globally emerging features of GRNs, such as functional redundancy, which can promote changes in network structure[3]; or (ii) local rewiring, which leads to the formation of new regulatory connections within GRNs[4]. The principles of GRN evolution have been primarily studied globally, at the level of entire networks, through comparative genomic analyses[4,5] or *in silico*[6,7], in order to understand how global network features determine evolutionary properties such as robustness[8] (phenotypic persistence in the face of mutation), tunability[9] (changes in gene expression levels) and evolvability[10] (capacity to acquire new regulatory connections). Yet, GRN structures can change solely through making and breaking of connections at the molecular level, that is, through local rewiring of individual components[11–16]. However, how characteristics of individual regulatory components impact on GRN evolution by determining robustness, tunability and evolvability is unknown.

Local network rewiring, that is, changes in the binding specificity of a TF, involves loss of binding, gain of binding and modifications in the strength of binding, which occur either through mutations in TFs or in DNA binding sites of TFs (operators). Most experimental studies on network rewiring have focused on mutations in proteins[17] or on the consequences of gene duplication events[18–20], showing that TF divergence affects GRN evolution[21]. However, in contrast to mutations in operators[22–24], mutational pathways of TFs are thought to be heavily constrained by epistasis between amino acids[25], the high frequency of deleterious mutations[26] and the strong pleiotropic effects of TFs[27], suggesting that operators are superior targets for modifying existing and acquiring novel network connections.

In contrast to previous studies on promoter evolution, which considered promoters independently of the associated TFs[24,28–30], we want to understand how the properties of a TF determine its evolutionary interactions with operator sites. To achieve this, we define the 'evolutionary potential for local rewiring' with respect to point mutations in an operator, thus characterizing the evolutionary potential for an individual network component that does not itself change: the repressor. We combine three distinct properties, which have been previously used to describe network rewiring[11,31,32], to define the evolutionary potential of a repressor as the ability (i) to withstand operator mutations (robustness), (ii) to modify the strength of binding to existing operators (tunability) and (iii) to acquire binding to new operators (evolvability) (Fig. 1a). Using two of the best understood prokaryotic repressors—Lambda CI and P22 C2—we study how characteristics of individual TFs determine the evolutionary potential for regulatory rewiring.

Results

Experimental system for quantitative measurements of evolutionary potential. We used homologous[33] elements of the bacteriophage Lambda and P22 genetic switches[34,35]. Specifically, we used Lambda CI and P22 C2 repressors, along with their respective P_R promoter regions. The P_R promoter region consists of RNA polymerase (RNAP) binding sites and two operators, O_{R1} and O_{R2}, which regulate P_R expression through cooperative repressor binding (Fig. 1b). We experimentally studied changes in gene expression, and hence binding of the repressors, along the mutational path between the two promoters by directionally mutating the operator sequence of one repressor to that of the other (Fig. 1c). Throughout, we refer to systems containing matching (non-matching) repressors and promoters as cognate (non-cognate) (Fig. 1b). We created a library of O_{R1} operator mutants by selecting all base pairs known to have large impact on repressor binding[36,37], and that differed between Lambda and P22 O_{R1} sequences, resulting in six mutated positions (Fig. 1d and Supplementary Table 1). Subsequently, we also investigated mutations in O_{R2}, even though repressor binding to this operator

[1]IST Austria, Am Campus 1, Klosterneuburg, Austria. [2]Institute of Integrative Biology, University of Liverpool, Liverpool, UK. [3]These authors contributed equally: Claudia Igler, Mato Lagator. *e-mail: calin@ist.ac.at

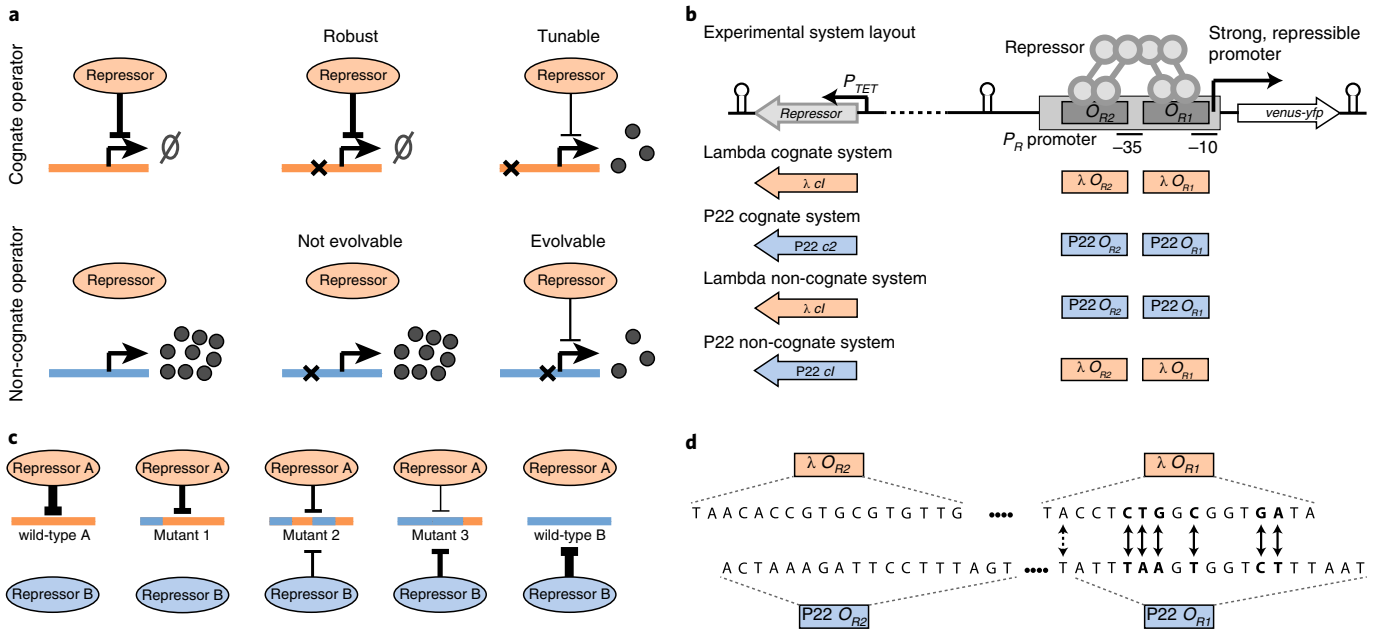

Fig. 1 | Experimental investigation of evolutionary potential of a repressor. a, Evolutionary potential of a repressor. Mutations (indicated by 'x') in the cognate operator can either have no effect on repressor binding (robust), alter repressor binding (tunable) or remove repressor binding (not shown). Mutations in the non-cognate site can either have no effect on repressor binding (not evolvable) or lead to gain of repressor binding (evolvable). Together, robustness, tunability and evolvability describe the evolutionary potential for regulatory rewiring. **b**, The synthetic template consists of a repressor controlled by an inducible P_{tet} promoter, and a strong P_R promoter—containing two repressor operators (O_{R1} and O_{R2}) and the RNAP binding sites—that controls the expression of a fluorescence marker *venus-yfp*. **c**, Experimental investigation of the evolutionary potential. An increasing number of mutations (blue) are introduced into the cognate operator (orange) of repressor A. The thickness of the blunt-ended arrows indicates the strength of repression. **d**, Mutated base pairs. Homology alignment of Lambda and P22 O_{R1} and O_{R2}, showing mutated sites in bold. Arrows show O_{R1} base pairs that were exchanged. The dashed arrow marks an additional site that was used to construct four cognate Lambda mutants, as one of the original positions abolished RNAP binding (Supplementary Table 1).

is considered to have only a minor direct impact on P_R repression[34]. All mutants were cloned into a very low copy number plasmid[38] and fluorescence as a proxy for P_R expression levels was measured in the presence and absence of repressor. This set-up, which measures binding of two repressors along the mutational path between the two operators, allowed us to study in a comparative manner how the evolutionary potential for regulatory rewiring depends on repressors themselves.

Evolutionary potential of repressors. To characterize the evolutionary potential of the two repressors, we experimentally measured their robustness, tunability and evolvability in terms of how repressor binding is affected by operator mutations. Robustness and tunability were quantified on the cognate promoter background. Robustness was the fraction of cognate operator mutants that maintained at least 90% repression. Tunability was the standard deviation in repression levels when repression was reduced but not completely lost (90−10%). From these definitions, it does not follow that robustness and tunability are necessarily negatively correlated: the expression variability (tunability) generated by non-robust mutations can be either large or small. Evolvability was the fraction of non-cognate operator mutants that could be repressed to at least 10%.

Lambda CI and P22 C2 have drastically different evolutionary potential (Fig. 2a), in spite of their shared ancestry[33]. These differences are particularly evident when considering the relationship between repression and the number of mutations in the operator (Fig. 2b). The high Lambda CI robustness to up to three mutations is surprising, since the O_{R1} site is almost fully conserved across at least 12 different lambdoid phages[39]. As this site is part of a complex promoter region in the phage, it could be conserved due to binding of RNAP or the second repressor in the switch (Cro). In contrast to Lambda CI, one to three mutations in the P22 cognate O_{R1} site led to a wide range of repression (0–100%).

At the non-cognate site, even introduction of single point mutations in P22 O_{R1} led to repression of at least 35% by Lambda CI (Fig. 2c). Gain of binding to the non-cognate site was much less frequent for P22 C2, and, except for one mutant, the range of repression was 0–20%, which is markedly lower than the 10–90% of Lambda CI (Fig. 2c).

Overall, Lambda CI had higher robustness as well as evolvability, suggesting that a repressor that is more robust to mutations in its cognate operator might also more readily acquire novel binding sites. At the same time, P22 C2 was more tunable, indicating a trade-off between robustness and tunability. The consistently stronger binding of Lambda CI compared to P22 C2 suggests that the evolutionary potential for regulatory rewiring is a property of the repressor, not of the operator.

Thermodynamic model of evolutionary potential. In order to expand on the experimental findings and identify how evolutionary potential depends on the biophysical system parameters, we used a thermodynamic model of gene regulation[40,41] (Fig. 3a). While experimentally we determined the general trends underlying the evolutionary potential of the two repressors by introducing mutations in a directional manner, we used the model to comprehensively explore all possible mutations in the six selected O_{R1} positions.

The model—for which all parameter values except repressor concentrations were taken from the literature (Supplementary Table 3 and Supplementary Fig. 1)—accurately reproduced experimental observations in cognate mutants (Supplementary Fig. 2).

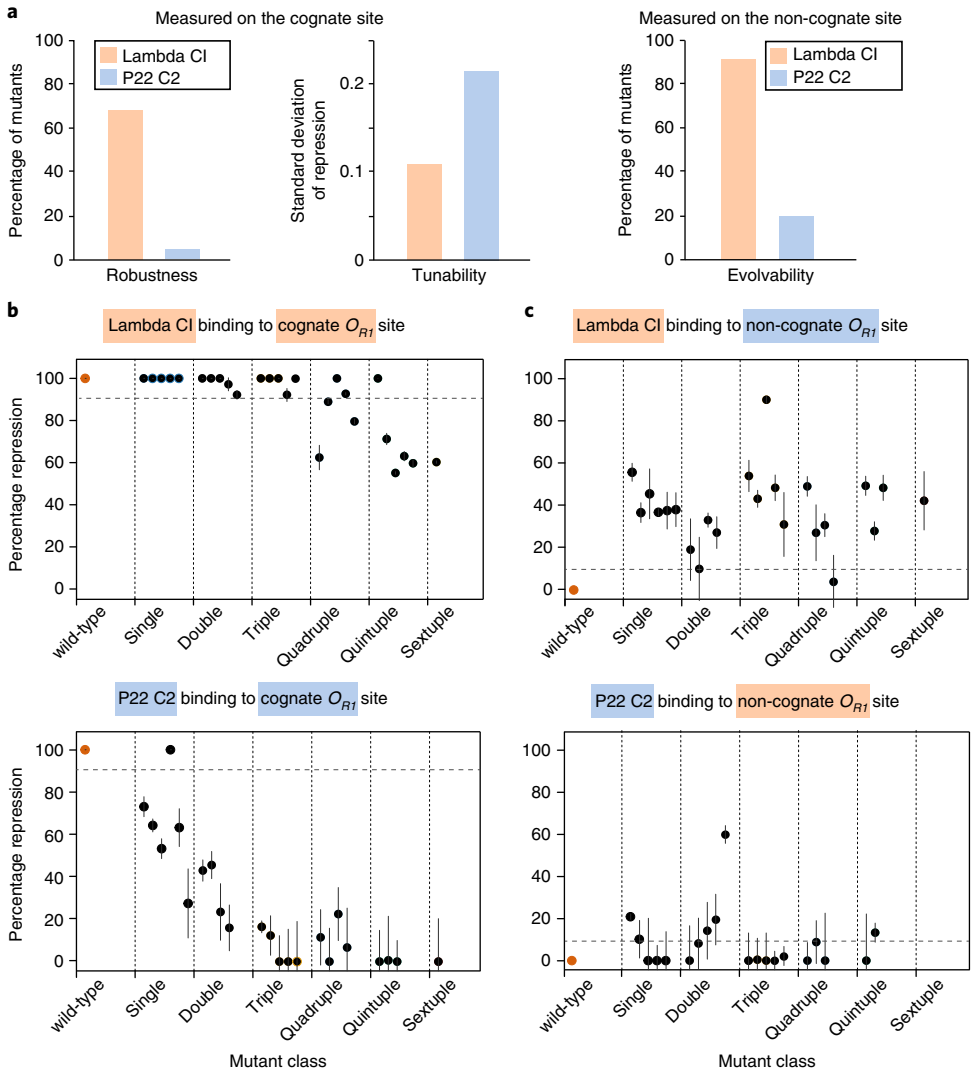

Fig. 2 | Lambda CI and P22 C2 have different evolutionary potential. a, Evolutionary potential of Lambda and P22 repressors. Robustness, tunability and evolvability of Lambda CI and P22 C2. **b**, Repressor binding to cognate mutants. Loss of binding was determined by mutating away from the cognate site, making it more similar to the non-cognate site. The dotted line shows the 90% repression threshold used to evaluate robustness. **c**, Repressor binding to non-cognate mutants. Gain of binding was determined by mutating away from the non-cognate site making it more similar to the cognate one. The dotted line shows the 10% repression threshold for evolvability. Expression levels in the absence of repressor are shown in Supplementary Table 2. Mutants that abolished RNAP binding are not shown, resulting in a different number of mutants in **b** and **c**. Points show mean percentage repression over three replicates and bars are standard errors of the mean. Lambda is orange and P22 is blue. Binding to the wild-type cognate or non-cognate site is shown by a dark orange point.

The poor model fit to non-cognate mutants is not surprising, as the model assumption of independent contribution of each position to the overall binding energy is known to be violated when mutated far away from the wild-type sequence[42]. Nevertheless, the use of the model is justified because the model performs comparably for both repressors (Supplementary Fig. 2), it provides a lower bound for the experimentally measured non-cognate repression and only modest improvements are achievable by accounting for dinucleotide dependencies[43,44].

We simulated binding to all possible mutants at the six chosen positions (4095) and quantified the evolutionary potential of repressors: for tunability and evolvability we used the same definitions as in the experiments (Fig. 3b,c), but calculated them separately for each mutant class. We used a standard definition to quantify robustness in our simulations[8] (see Methods), which we could not apply to the experimental measurements due to the insufficient number of mutants connected by single mutations. Importantly, applying the experimental definition of robustness to the simulations identified consistent differences in robustness (51.9% for Lambda CI and 0.3% for P22 C2). Overall, model simulations corroborated the experimentally determined differences in the evolutionary potential of the two repressors: Lambda CI was more robust and more evolvable than P22 C2, but less tunable for up to three mutations (Fig. 3d).

To confirm that the observed differences in the evolutionary potential did not arise from the specific operator sites used in this study, we simulated the evolvability of both repressors to 10^6 random operators. We found that Lambda CI bound a consistently higher portion of random sites (Supplementary Fig. 3) irrespective of repressor and RNAP concentration, further supporting the view that evolutionary potential is a property of the repressor, not the operator.

The thermodynamic model identifies several system parameters that affect the evolutionary potential of a repressor (Fig. 3a): (i) intracellular conditions, that is, concentrations of repressor

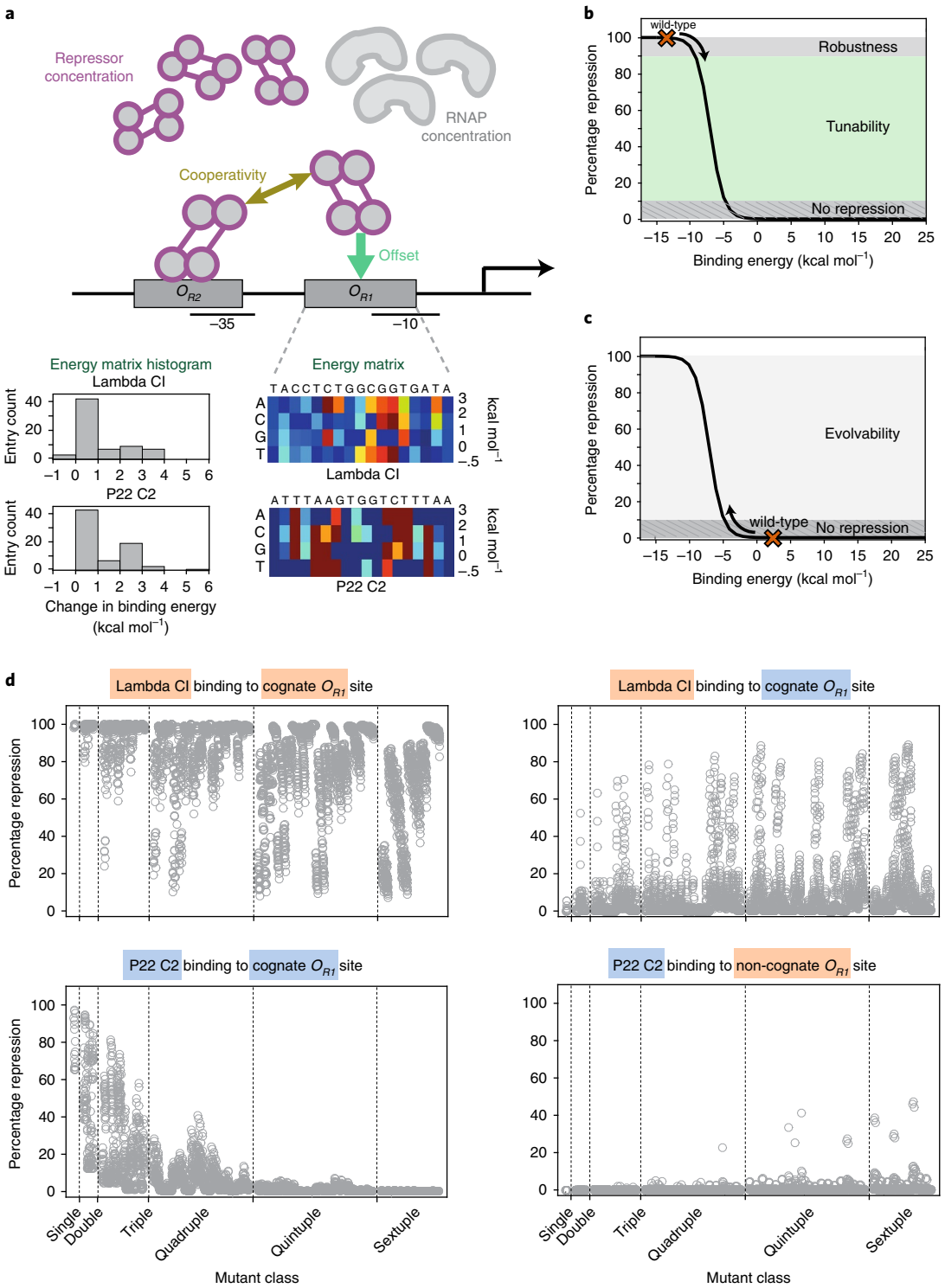

Fig. 3 | Thermodynamic model of gene expression. a, Parameters affecting evolutionary potential. Gene expression is determined by: intracellular concentration of (i) repressor and (ii) RNAP; (iii) cooperativity of binding between two repressor dimers; (iv) binding energy to the wild-type operator (offset E_{WT}); and (v) additional contribution of each mutation to the binding energy (energy matrix). Negative (positive) entries in the energy matrix show mutations that decrease (increase) binding energy, and hence increase (decrease) repression. Zero values denote the wild-type sequence. **b**, **c**, Robustness and tunability (**b**), and evolvability (**c**). The sigmoidal relationship between binding energy and repression, determined by the thermodynamic model, provides quantitative definitions of robustness, tunability and evolvability. **d**, Comprehensive computational exploration of the evolutionary potential of Lambda CI and P22 C2. Comprehensive simulation of repression for all possible mutations in the six chosen positions in O_{R1}.

and RNAP; (ii) interactions arising from the promoter architecture, which in our system enable cooperative repressor binding; and (iii) intrinsic binding characteristics of the repressor itself. Repressor-specific binding characteristics are captured in the total binding energy, E_{tot}, which is determined by the strength of repressor binding to its wild-type operator (called the 'offset' or E_{WT}), to

a

	Robustness	Tunability	Evolvability
Repressor concentration (range: 1–7 × 10^{-6}M)	+ / +	− / *	+ / +
RNAP concentration (range: 1–7 × 10^{-6}M)	0 / −	+ / *	− / −
Cooperativity (range: 1–7 k_BT)	+ / +	− / *	n/a

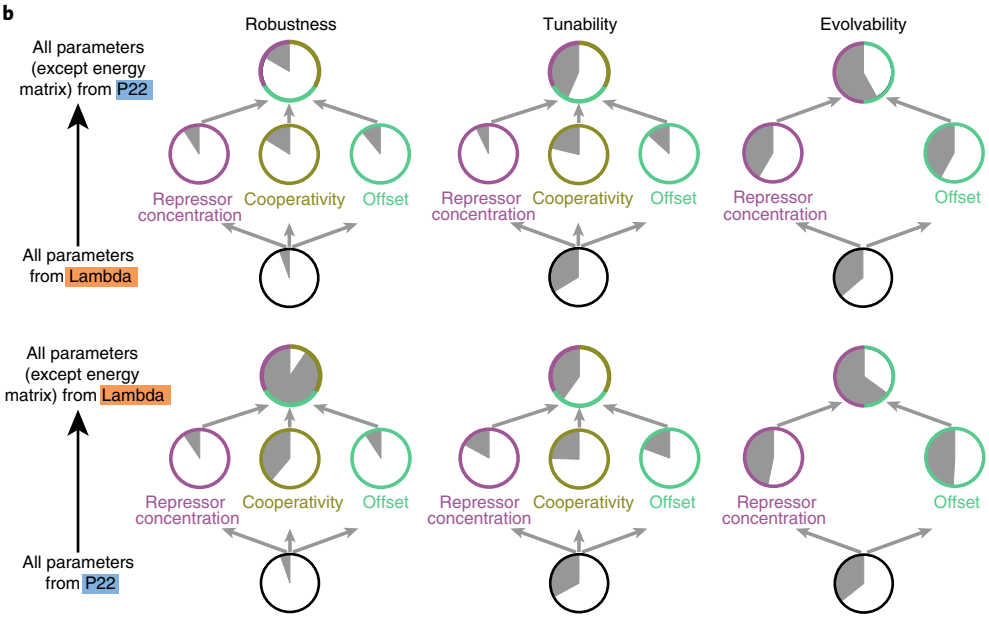

Fig. 4 | System parameters determine evolutionary potential. a, Effects of repressor concentration, RNAP concentration and cooperativity on evolutionary potential. Correlation between each evolutionary property and a given system parameter: '+' indicates a positive correlation; '−' a negative correlation; '0' a negligible effect; and '*' a non-linear relationship. n/a indicates that the absence of a cognate O_{R2} site prevents binding cooperativity. Lambda CI is orange and P22 C2 is blue. **b**, Swapping model parameters between Lambda CI and P22 C2. We swapped parameter values of repressor concentration, cooperativity and offset from one repressor to the other. 'Fraction of variance explained' (R^2) was calculated between the repressor with swapped parameter(s) and the other repressor with its original parameters. R^2 is shown as the grey portion of the pie charts: the fuller the pie chart, the more similar the evolutionary property between the two repressors. Starting from the original parameter values, each of the three parameters was swapped individually and all three simultaneously.

which the effect of each mutation on binding is added, as defined by the 'energy matrix' (E_{seq}), so that $E_{tot} = E_{WT} + E_{seq}$. Hence, the offset captures the overall propensity of a repressor to bind cognate DNA, while the energy matrix describes how operator mutations affect repressor binding.

Repressor and RNAP concentrations, as well as binding cooperativity, influence robustness, tunability and evolvability to different degrees, although not always in a straightforward manner (Fig. 4a and Supplementary Figs. 4–6). As such, the evolutionary potential for rewiring depends on intracellular conditions that change with cellular physiology[45], and on the promoter architecture that can determine binding cooperativity. Experimental measurements of relative repressor concentrations revealed 3.8- to 5.5-fold higher intracellular Lambda CI levels (Supplementary Fig. 1). Reassuringly, the difference in evolutionary potential between repressors was consistently identified across a range of repressor and RNAP concentrations, making the model results largely independent of uncertainty in these parameters (Supplementary Fig. 7).

Biophysical determinants of evolutionary potential. We asked if it was possible to reconcile the differences in the evolutionary potential between Lambda CI and P22 C2 by swapping their model parameters. Specifically, we calculated robustness and tunability for one repressor after swapping either repressor concentration or cooperativity with the parameter values of the other repressor. For evolvability, we only swapped repressor concentration, since the absence of a cognate O_{R2} site prevented cooperative binding.

Swapping either repressor concentration or cooperativity between Lambda CI and P22 C2 decreased the differences in robustness and evolvability, but still left a disparity in robustness, tunability and evolvability of at least 50% (Fig. 4b). Therefore, intrinsic binding characteristics of repressors—the offset and the energy matrix—crucially determine their evolutionary potential, as previously found for the regulation of the *lac* promoter[46]. When we swapped the offset between the two repressors, we found that the effect was comparable to the effects of swapping either repressor concentration or cooperativity. Notably, swapping all three parameters did not lead to a full reconciliation between the two repressors (Fig. 4b), indicating that the energy matrices accounted for the remaining differences of at least 30% (except for robustness when swapping from P22 C2 to Lambda CI).

To better understand the mechanism by which intrinsic binding characteristics of a repressor (offset and energy matrix) determine the differences in the evolutionary potential, we developed an intuitive and generic description of robustness, tunability and evolvability based on the sigmoidal curve relating repressor binding energy to repression (Fig. 5a). The formulas in Fig. 5a describe the evolutionary potential in terms of the offset and the energy matrix, rather

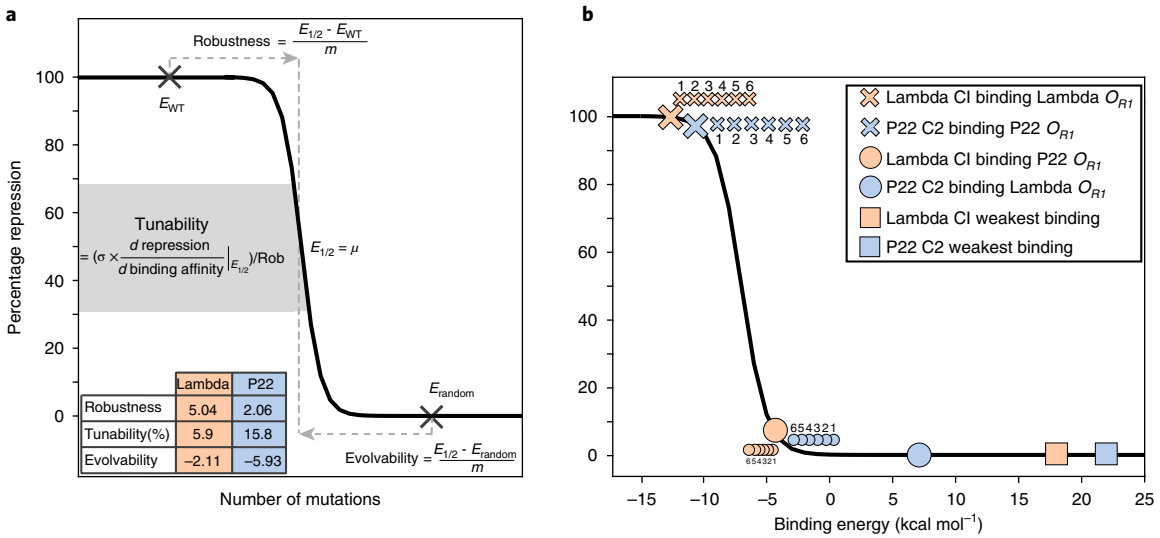

Fig. 5 | Biophysical determinants of the evolutionary potential. a, Generic descriptions of the evolutionary potential. Generic definitions of robustness, tunability and evolvability that use only the offset and the energy matrix. Rob = $\frac{E_{1/2} - E_{WT}}{m}$ and Evo = $\frac{E_{1/2} - E_{random}}{m}$ = Rob + #mut, in which $E_{1/2}$ is the binding energy at half-repression (which equals the chemical potential, μ), E_{random} is the typical binding energy to a random sequence, m the average mutational effect size and *#mut* the distance of the random sequence to the cognate operator in number of mutations (see Methods). Evolvability is negative as mutations towards $E_{1/2}$ improve binding. Tun = $\left(\sigma \times \frac{d\ \text{repression}}{d\ \text{bindingaffinity}}\Big|_{E_{1/2}}\right) / \text{Rob}$, where σ is the standard deviation of the energy matrix and $\frac{d\ \text{repression}}{d\ \text{bindingaffinity}}|_{E_{1/2}}$ the slope of the sigmoid curve at $E_{1/2}$. The table shows the values for robustness, tunability and evolvability for the experimental systems (Fig. 1b). Here we calculated evolvability for the non-cognate sites of Lambda CI and P22 C2. **b**, Energy matrix and offset determine the evolutionary potential. Locations of Lambda CI and P22 C2 binding to three categories of operators (E_{WT}, $E_{non\text{-}cognate}$, E_{max}) are indicated by large symbols on the sigmoidal curve relating binding energy and repression. Repressor concentrations are kept equal. Small symbols show mean energy values obtained through model simulations for different mutant classes (1, single; 2, double; and so on) when mutating the cognate (crosses) or the non-cognate (circles) operators.

than using the full thermodynamic model. Robustness is the average number of mutational steps needed to lose 50% of repression. Evolvability is the average number of mutational steps necessary to gain 50% of repression starting from a given random sequence. Tunability is the ease of generating variation in gene expression levels, that is, the variation in repression around the half-repression point, defined in relation to the distance between this point and the cognate operator (Fig. 5a).

Adopting these generic definitions results in simple analytical expressions (Fig. 5a), which show that robustness and evolvability are positively correlated through the number of mutations that separate the given random sequence from the cognate operator. This correlation holds true as long as: (i) the average mutational effect size (m) is relatively small and similar between repressors—which is a reasonable assumption in general because the scale of m is set by the energetics of hydrogen bonds (1–3 kcal mol^{-1})[47], but also an assumption that is specifically testable for any particular set of TFs for which the energy matrices are known; and (ii) the energy matrix is a fixed property of a repressor, meaning that m stays constant when mutating towards a random non-cognate site. Tunability, on the other hand, is in a trade-off with robustness, although the dependence of tunability on the standard deviation of mutational effects suggests that this relationship can be adjusted to some extent.

Applying these generic definitions to the systems used in this study, we observe higher robustness and evolvability, but lower tunability for Lambda CI (Fig. 5a). To illustrate that these generic definitions are in accordance with the binding landscape obtained through model simulations, we used the simplest model set-up where repressors bind only a single operator site and repressor concentrations are the same. We selected three operator sequences for each repressor—the cognate (E_{WT}), the non-cognate ($E_{non\text{-}cognate}$) and the weakest binding (E_{max}) sequence—computed their binding energies and positioned them on the sigmoidal repression curve.

The consistently stronger binding of Lambda CI to all three types of operators (Fig. 5b) arises from its lower offset (−13.2 kcal mol^{-1}, compared to −12 kcal mol^{-1} for P22 C2) and smaller average mutational effect size (1.23 kcal mol^{-1}, compared to 2.43 kcal mol^{-1} for P22 C2). Positioning the mean binding energy of each mutant class (Fig. 2) on the sigmoidal curve (hence not using the full model but only the offset and the energy matrix) allowed accurate predictions of the experimental measurements, at least for cognate sites (Supplementary Fig. 8). Therefore, the lower offset of Lambda CI places it further away from the slope of the repression curve (Fig. 5b), resulting in higher robustness, but lower tunability. Similarly, Lambda CI binds the non-cognate operator, all of its mutants and even the operator sequence with weakest possible binding more strongly (Fig. 5b), illustrating that, on average, Lambda CI binding a random sequence will be closer to the rise of the sigmoidal curve and hence more evolvable.

Role of inter-operator epistasis. We investigated experimentally if promoter architecture—the existence of multiple operator sites—can affect the observed trade-off between robustness/evolvability and tunability. We first tested the effects of mutating four residues in the Lambda cognate O_{R2} (Supplementary Table 4). The effects of mutations in O_{R2} on repression (Fig. 6a) were modest (75–100% repression), but less robust than mutations in O_{R1} (comparing Fig. 6a to Fig. 2b, top panel), despite the supposedly weaker influence of O_{R2} on repression[34].

We tested for interactions between mutations in two operators (inter-operator epistasis) by creating a cognate library with mutations in both O_{R1} and O_{R2}. Because the trade-off between high robustness and low tunability was observed only in Lambda CI, we focused only on inter-operator epistasis in the cognate Lambda system. We randomly selected three neutral O_{R1} mutants and combined each with eight randomly selected O_{R2} mutants (Supplementary Tables 1

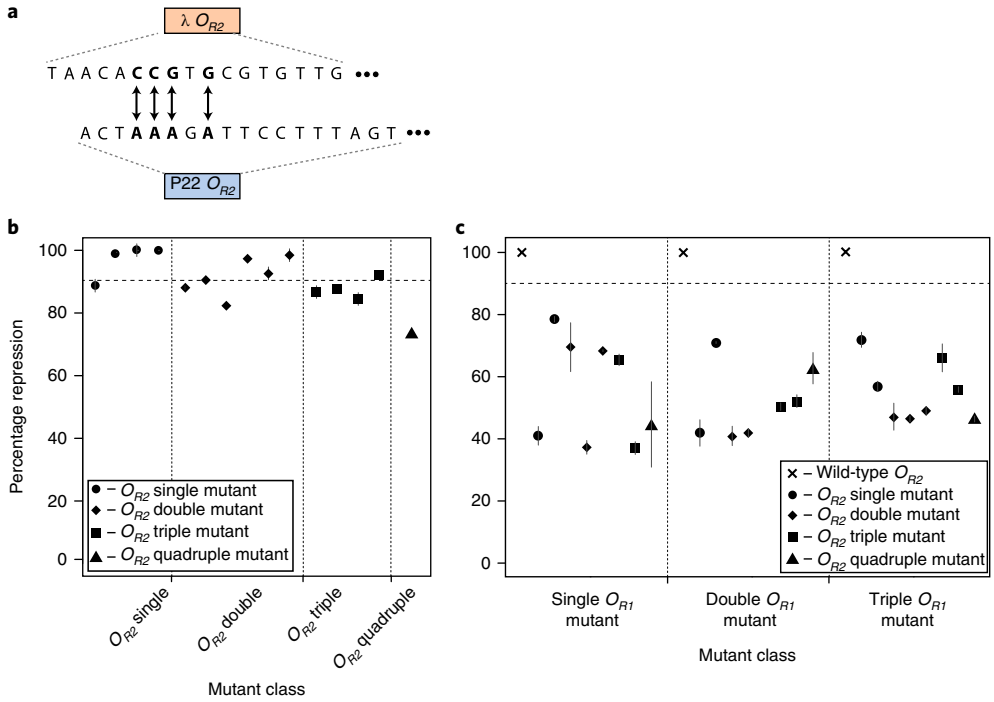

Fig. 6 | Inter-operator epistasis alleviates the trade-off between robustness and tunability. a, Mutated base pairs in Lambda O_{R2}. Homology alignment of Lambda and P22 O_{R2}, showing mutated sites in bold. Arrows show base pairs that were exchanged between the two operators (Supplementary Table 4). **b**, **c**, Lambda CI binding to cognate O_{R2} mutants (**b**) and Lambda CI binding to cognate O_{R1} and O_{R2} mutants (**c**). Loss of Lambda CI binding due to mutations in cognate O_{R2} (**b**) and both cognate sites (**c**). Points are mean percentage repression of three replicates and bars are standard errors of the mean. Plot symbols indicate O_{R2} mutant class. 'x' symbols correspond to the operator with the given O_{R1} mutation(s) and the wild-type O_{R2} sequence (Fig. 2b). One O_{R1}–O_{R2} mutant gave no measurable expression in the absence of repressor and is not shown.

and 4). We observed a wider spectrum of repression values (40–80%), and hence higher tunability, among these mutants (Fig. 6b) compared to mutations in individual operators (Supplementary Table 5). This meant that mutations in O_{R2} exacerbate the effects of phenotypically neutral O_{R1} mutations, indicating pervasive inter-operator epistasis (Supplementary Table 6). Inter-operator epistasis arising from multiple mutations in both operators could not be captured by the thermodynamic model (Supplementary Fig. 9), which is in contrast to a previous study where we introduced only a single point mutation into each operator[48]. However, the findings we report here are in line with studies showing that the presence of multiple operators can obstruct sequence-based predictions of gene expression[49].

Inter-operator epistasis alleviated the trade-off between robustness and tunability for Lambda CI in O_{R1}, probably by effectively modifying cooperative repressor binding. This role of inter-operator epistasis could be specific to operators that are functionally connected through cooperative binding and might be different for redundant operators. Our results suggest that, for cooperative binding, additional operators can facilitate network rewiring, as inter-operator epistasis helps generate expression level diversity, while maintaining robustness to the existing operators.

Discussion

The principles that govern gene regulatory evolution, which have been studied primarily from a global network perspective, remain poorly understood. Here, we identify the biophysical mechanisms that determine the evolutionary potential of transcription factors for rewiring of regulatory network connections. Specifically, we provide an analytical expression (Fig. 5a) that, under reasonable assumptions, correlates robustness, tunability and evolvability (as defined in this study). Indeed, we experimentally observed these correlations for two closely related repressors: Lambda CI is more robust and at the same time more evolvable, while P22 C2 is more tunable. These differences in mutational effects probably arise from differences in specific DNA binding mechanisms[50]: while the binding specificity of Lambda CI is mostly based on direct contacts between operator bases and amino acid residues[36], the affinity of P22 C2 relies strongly on the local DNA conformation[37,51]. The non-linear relationship between binding energy and repression, which is inherent to the thermodynamic model[52] (Fig. 3), captures the differences in robustness, tunability and evolvability, explaining how the intrinsic binding characteristics of a repressor determine its evolutionary potential for regulatory rewiring (Fig. 5). The model does so by representing the evolutionary potential for each repressor through its total binding energy (offset E_{WT} plus energy matrix E_{seq}) and the average effect size of mutations (given by the energy matrix). Typically, energy matrices are used to determine and predict binding of TFs to a given DNA sequence[53]. However, our findings imply that the composition of the energy matrix crucially determines not only the current regulatory structure, but also the potential of the repressor to contribute to GRN evolution through making and breaking of individual connections. It is worth noting that while we only considered steady-state expression levels, operator mutations could also affect expression dynamics, which might be subject to different constraints.

The *in vivo* positive correlation between robustness and evolvability is surprising, as molecular systems that are more persistent in the face of mutational pressure are generally assumed to be less likely to acquire novel functions[54]. Previous theoretical studies attempted to resolve this paradox by describing how robustness and evolvability 'emerge' as properties of existing networks[3,8,55,56], but so far, direct experimental approaches have been missing. We experimentally resolve this apparent paradox by showing that local mechanisms of TF–DNA binding intrinsically correlate robustness

and evolvability in a positive manner. In fact, this positive correlation can be explained through an analytical expression that shows how robustness and evolvability are connected through the mutational distance between the cognate operator and a random DNA sequence (Fig. 5a). As such, a more promiscuous TF is simultaneously more robust and more evolvable, retaining cognate binding more easily while facilitating acquisition of novel operator sites. The positive correlation between robustness and evolvability can facilitate GRN evolution[19] by enabling a neutral network of genotypes, throughout which mutations have small phenotypic consequences[3,8]. Lambda CI is known to be promiscuous, showing non-specific binding across the *Escherichia coli* genome[57] and to non-cognate phage operators[58]. Thus, a Lambda CI-like TF has a higher potential to become a global regulator, whereas a P22 C2-like TF would be more suited as a local regulator, since its easy loss of binding could facilitate rewiring by reducing detrimental crosstalk[59]. However, the same biophysical mechanisms can impose a trade-off between evolvability and tunability, thus constraining the range of expression levels that can be achieved by a promiscuous TF at a single operator.

Given the key role that rewiring of local regulatory connections plays in changing GRN structure, the scarcity of direct experimental approaches studying the mechanisms of rewiring is striking. Our work provides a mechanistic link between the biophysics of TF–DNA binding and GRN evolution. Epistatic interactions, which emerge through the presence of multiple operators and alleviate the trade-off between tunability and robustness/evolvability, can prevent a straightforward prediction of how local rewiring properties determine global network evolution. Moreover, the binding landscape for regulatory rewiring we describe is based purely on biophysical characteristics that connect genotype (mutations) to phenotype (gene expression levels), which will be further shaped by selection forces acting on this landscape[29,30,60]. By integrating biophysical models with the existing molecular knowledge of regulatory elements, our work provides the first steps towards a quantitative mechanistic framework for understanding gene regulatory network evolution.

Methods

Strains and plasmids. The experimental system is based on the 'genetic switches' of the bacteriophages Lambda and P22, which have similar regulatory architecture and substantial structural homology due to shared ancestry[33]; specifically we use the P_R promoter system. We constructed a template plasmid consisting of two parts that are separated by 500 random base pairs and a terminator sequence (represented by a hairpin structure in Fig. 1b): an inducible repressor gene on one strand and a regulatory region controlling a fluorescence marker on the other strand. Either Lambda CI or P22 C2 were placed after an inducible P_{TET} promoter. The fluorescent protein gene *venus-yfp*[61] was placed under the control of the P_R regulatory promoter region, containing an RNAP binding site as well as two operators, O_{R1} and O_{R2}, either from Lambda or P22. Specifically, for Lambda P_R we used the region from −60 bp upstream of the transcriptional start site to +9 bp downstream. The specific location of the transcriptional start site for P22 P_R has not been defined. Therefore, upstream of O_{R2} and downstream of O_{R1} we used the wild-type P22 sequence that was of the same bp length as the analogous Lambda P_R regions. This meant that we used the wild-type P22 sequence from −65 bp upstream up to the start codon of *cro*. O_{R1} more strongly binds the repressor and is in direct overlap with the RNAP binding site (−10). O_{R2} has a weaker affinity for the repressor and assists in repression mainly through cooperative binding between two repressor dimers[62]. Downstream of the phage sequences both promoter regions contain the same ribosomal binding site in front of the reporter gene. These parts were cloned in all four combinations (cognate combinations: Lambda *cI* with Lambda P_R and P22 *c2* with P22 P_R; non-cognate combinations: Lambda *cI* with P22 P_R and P22 *c2* with Lambda P_R) into a low copy number plasmid (pZS*) containing a kanamycin resistance marker[38]. The TL17 terminator sequences followed the repressor genes and the T1 terminator the *venus-yfp* (Fig. 1b). The plasmid libraries were then transformed into MG1655 derived *E. coli* cells (strain BW27785, CGSC (Coli Genetic Stock Center) no.: 7881)[63].

Construction of mutant O_{R1} libraries. We created a library of mutants in O_{R1} by selecting six base pairs that were found to be most important for the binding of either of the two repressors[36,37], and that differed between Lambda and P22 O_{R1} sequences. This was done by aligning the O_{R1} sites from Lambda and P22 wild-type operators (according to homology, not symmetry) and comparing the corresponding base pairs in the operator sites. The six base pairs that were most important for repressor binding and that differed between the two operators were substituted by the base pairs of the non-cognate O_{R1} in both directions: starting with wild-type Lambda O_{R1} and mutating it to be more similar to P22 O_{R1}; as well as starting with wild-type P22 O_{R1} and mutating it to be more similar to Lambda. We generated all six single mutants, four double, five triple, four quadruple, three quintuple and the sextuple mutant. For mutating Lambda O_{R1} from cognate to non-cognate, ten additional mutants were constructed that did not contain mutations in base pairs overlapping the −10 binding region of RNAP: two double, two triple, two quadruple, three quintuple,and another sextuple mutant. For the quintuple and sextuple mutants an additional base pair was chosen that was linked to high affinity binding of Lambda CI (Supplementary Table 1). The additional double and triple mutants were also created for the P22 non-cognate library. O_{R1} operator libraries were constructed by synthesizing oligos of 73 bp length (Sigma Aldrich), carrying wild-type O_{R2} and mutated O_{R1} (Supplementary Table 1) and cloning them into the experimental system plasmid backbone (Fig. 1b). Clones carrying correct mutants were confirmed through Sanger sequencing.

We also tried to construct promoter regions containing cognate O_{R1} and non-cognate O_{R2}. As both operators contain parts of the RNAP binding site, we did not obtain fluorescence expression in the absence of CI from these promoters even when we varied the spacing between the operators. This is possibly due to factors other than sequence-dependent binding energy playing a role in the regulatory context of these promoters[49].

Fluorescence assays. We measured fluorescence of all O_{R1} mutants (Lambda and P22 cognate and non-cognate systems), both in the presence and in the absence of the inducer aTc. Three biological replicates of each mutant of the library were grown at 37 °C overnight in M9 media, supplemented with 0.1% casamino acids, 0.2% glucose, 30 μg ml^{-1} kanamycin, and either without or with 15 ng ml^{-1} aTc. Overnight cultures were diluted 1,000×, grown to $A_{600\,nm}$ of approximately 0.05 and their fluorescence measured in a Bio-Tek Synergy H1 plate reader. All replicate measurements were randomized across multiple 96-well plates. All measured mutants had fluorescence levels significantly above the detection limit of the plate reader, resulting in measurements at least 1.5-fold greater than the non-fluorescent control.

Fluorescence values were normalized by $A_{600\,nm}$ values (in relative fluorescence units, RFU) and averaged over three replicates. Repression values were calculated as a normalized ratio between the measured fluorescence with and without the repressor:

$$\text{Percentage repression} = \left(1 - \frac{\text{RFU}_{\text{repressor}}}{\text{RFU}_{\text{norepressor}}}\right) \times 100.$$

Standard errors of the mean repression values were calculated using error propagation in order to account for the inherent variability in the fluorescence measurements. The fluorescence levels measured in the absence of repressor were comparable across all Lambda operator mutants, as well as all P22 operator mutants (Supplementary Table 2). This means that the reported differences in percentage repression arose mainly from changes in repressor binding, rather than alterations to the RNAP binding site. Moreover, our simulations showed that changes in RNAP concentration, which correlates with the strength of RNAP binding, do not change the qualitative pattern of binding for the two repressors. Interestingly, when compared to P22 wild-type O_{R1}, all of the P22 cognate O_{R1} operator mutants showed increased expression levels in the absence of repressor. Lambda P_R is a stronger promoter than P22 P_R and introducing mutations in the operator region of P22 P_R increased promoter strength by making it more similar to Lambda P_R.

Direct comparisons between the in vivo effects of operator mutations on gene expression level that we measured and the previous published studies of the same operators[36,37] were hindered by the in vitro nature of previous studies. All previous studies of Lambda P_R and P22 P_R mutants relied on biochemical filter binding assays, which do not account for cooperativity between the two sites, and as such do not necessarily translate quantitatively into gene expression levels. As such, comparisons between published and our data are possible only through a modelling framework, such as the one we utilize (see Methods section, Thermodynamic model of repression at the P_R promoter).

For the experimental data, the evolutionary properties were calculated in the following way. Robustness and tunability of the repressors were evaluated on the cognate operator mutants. Robustness for the experimental data was calculated as the percentage of mutants for which >90% of the wild-type repression was retained. Tunability was calculated as the standard deviation in repression levels for mutants that exhibited between 10% and 90% of the wild-type repression. On the cognate background, mutants that were repressed less than 10% were considered neither robust nor tunable. Evolvability was calculated as the portion of non-cognate mutants that were repressed to more than 10%.

Cellular concentrations of the two repressors were determined using western blots. Lambda CI and P22 C2 were cloned with a His-Tag or an HA-Tag,

respectively, at their carboxy-terminal end. Rat and rabbit primary antibodies (Roche and Thermo Fisher, respectively) in combination with goat anti-rat and anti-rabbit secondary antibodies (Thermo Fisher) were used to detect them. Samples were processed once at full concentration and once at 2-fold dilution. The obtained bands from gel electrophoresis were normalized by a household gene and normalized concentrations between the two repressors were compared as $\left(\frac{\text{concentration}_{\text{Lambda CI}}}{\text{concentration}_{\text{P22 C2}}}\right)$. Lambda CI was present in excess over P22 C2: 3.8-fold for full concentration samples and 5.5-fold for diluted samples. We also tested variation in repressor levels by measuring fluorescence from the P_{TET} promoter on the same plasmid construct as used in the library measurements for six replicates either without or with 15 ng ml^{-1} aTc and found only minor variability (without aTc: 3.6% CV, with aTc: 2% CV) that cannot explain the experimentally observed differences between the repressors.

Thermodynamic model of repression at the P_R promoter. The model is based on previously described thermodynamic approaches[40,41], which rely on several assumptions: (i) TF binding to DNA takes place at thermodynamic equilibrium; (ii) gene expression can be equated with the probability of binding of participating proteins (in our case RNAP and repressor); and (iii) the contribution of each base pair in the operator to binding is additive. The probability of a gene being expressed is derived by summing the Boltzmann weights over all promoter occupancy states where RNAP is bound. Boltzmann weights are given by $w_i = [N]^* e^{(E_{\text{tot}} - \mu)}$, where E_{tot} is the energy of a certain configuration, N is the molecule concentration (in μM) and μ is the chemical potential. E_{tot}, the total binding energy, is composed of the offset (E_{WT}), which is the energy of binding to a reference (wild-type) sequence; and the binding energy derived for a specific sequence from the energy matrix of the binding protein $E_{\text{seq}} = \sum_{i=1}^{l} \epsilon_i(a_i)$, where l is the length of the sequence, a_i the specific nucleotide at position i and ϵ_i the energy contribution due to the energy matrix of the specific nucleotide a at position i. Total binding energy is therefore $E_{\text{tot}} = E_{\text{WT}} + E_{\text{seq}}$. Binding energies and chemical potential are given in kcal mol^{-1}. In our model system, there are two operator sites (O_{R1} and O_{R2}) that can each be occupied by a repressor dimer, and binding to each operator site is affected by the strength of cooperative binding between them. The probability of the gene being expressed is then given by the sum of all states conducive to promoter expression (RNAP bound) normalized by the sum over all possible states:

$$\text{Gene expression} = \frac{1}{1 + \frac{K_p}{[\text{RNAP}]} \frac{\left(1 + 2\frac{[R]}{K_R} + \left(\frac{[R]}{K_R}\right)^2 \epsilon^{\omega}\right)}{\left(1 + \frac{[R]}{K_R}\right)}},$$

where $K_x = e^{(E_{\text{tot},x} - \mu)}$ represents the effective equilibrium dissociation constant (relative to the genomic background)—which is the concentration for half-maximal occupation of the site—of, either RNAP (K_p) or the repressor (K_R). We simplified this formula by not distinguishing between different binding affinities of repressors for O_{R1} and O_{R2}. Please note that we account for concentration-specific effects separately and μ incorporates only non-specific background binding and other unspecific cellular effects. The probability of transcription factor (TF)–DNA binding is of the form[22]: $p_i = \frac{[\text{TF}_i]/K_i}{1 + [\text{TF}_i]/K_i}$. Based on Gerland et al.[23], we can assume that K_x is individually tunable for each binding site. $[R]$ is the concentration of repressor dimers, which is the effective concentration, as repressors only bind as dimers and, as we assume fast dimerization[64], this corresponds to half of the total monomer concentration in the cell. [RNAP] is the concentration of RNAP and ω is the cooperativity energy value, describing the strength of interaction between two repressor dimers. All concentrations and dissociation constants are given in units of μM. The calculated gene expression value is a relative measure, with 1 indicating full expression and 0 no expression. Percentage repression was then calculated using the formula

$$\text{Percentage repression} = \left(1 - \frac{\text{gene expression}_{\text{repressor}}}{\text{gene expression}_{\text{no repressor}}}\right) \times 100.$$

In the 'main model', which is used throughout the study, RNAP competes with repressor binding at O_{R1} and repressor binding to O_{R1} is increased by cooperative binding of a second dimer to O_{R2}. Therefore, the following scenarios are possible: (i) the promoter can be bound by neither protein; (ii) RNAP can be bound either alone or together with the repressor at O_{R2}; or (iii) the repressor bound to O_{R1} keeps RNAP from binding, either by binding on its own or cooperatively together with another repressor at O_{R2}. The corresponding formula was taken from Bintu et al.[40] (Case 4). We also considered an 'alternative model' where O_{R2} binding impedes RNAP binding as well (Bintu et al.[40]; Case 6), but as the main model always gave a better fit to experimental data, we utilized only the main model throughout.

Energy values for binding to mutated sequences were calculated for RNAP and repressor binding using the respective energy matrices by adding up the individual relative contributions of each base pair and adding an offset. The offset is the energy of binding of the repressor to the wild-type sequence, which was added because the energy matrix calculates only energy differences relative to wild-type binding. Binding energy matrices were based on Sarai and Takeda[36] for Lambda CI, on Hilchey *et al.*[37] for P22 C2—which were both determined biochemically—and, for RNAP, on an ongoing work on RNAP binding to Lambda P_R within the group. Wild-type binding affinities of Lambda CI to both operators (offset) were taken from Vilar[67]. Other model parameters were taken from the following sources: binding cooperativity and non-specific binding energy were adopted from Hermsen *et al.*[69]; wild-type binding affinities for both operators were obtained from Hilchey *et al.*[37] for P22 repressor; and binding energy and concentration for RNAP were taken from Santillan and Mackey[65]. Promoter strength for both Lambda P_R and P22 P_R was based on previously published values for the Lambda P_L promoter[66], but we also found that the results were not sensitive to this parameter. Repressor dimer concentrations were the only parameters that were fitted to the data by means of a Monte Carlo algorithm. The algorithm used simulated annealing to find the optimal parameter values minimizing the squared difference between the predicted and observed percentage repression between the data and the model. The fitted difference in concentration values between the two repressors is slightly lower than found experimentally (Supplementary Fig. 1). We tested the model for concentration values from 0- to 7-fold difference and always found the same trends in the evolutionary potential (Supplementary Fig. 7). Note that standard experimental measures cannot provide effective TF concentrations (that is, proteins that are free to bind at the target site), especially when two TFs are not equally promiscuous, as these measures cannot distinguish free and non-specifically bound proteins. Because of this, and because the overall differences in evolutionary potential did not depend on variations in repressor concentration parameters, we used repressor concentrations determined by the best model fit and not those we experimentally measured. All parameter values used in the model are shown in Supplementary Table 3.

In order to verify the fit of our model to the experimental data, linear regression was performed between the data obtained experimentally (see Fluorescence assays) and the prediction of repression values produced through the thermodynamic model. Matlab R2015a software was used to calculate the regression, R^2 and P values for the O_{R1} library (Supplementary Fig. 2). The model accurately reproduced experimental observations in cognate mutants, but did not fit non-cognate mutant measurements (Supplementary Fig. 2). The lack of fit to non-cognate mutants is not surprising, as thermodynamic models assume an independent contribution of each position, which does not hold when mutated far away from the wild-type operator sequence[42,67]. Nevertheless, because the model provided a lower bound on the experimentally measured non-cognate repression levels (Supplementary Fig. 2), we used it to explore parameters affecting repression at non-cognate sites as well.

Robustness. Robustness was calculated for repressors binding to cognate mutants only if they retained more than 20% repression. We counted the number of robust neighbours for each operator, where 'robust neighbour' refers to an operator sequence that is exactly one mutation away from the reference and exhibits more than 90% repression of the reference repression value. Specifically, starting from the wild type, each mutant (above the 20% repression threshold) was taken as a reference and repression of all other mutants that are exactly one mutation away was calculated. The relative count of robust neighbours was averaged for each reference operator and the mean was taken over each mutant class. This procedure was repeated with different values for cooperativity (1,3,5,7 kcal mol^{-1}), repressor concentration (1,3,5,7 μM) and RNAP concentration (1,3,5,7 μM). We tested if the results were sensitive to the percentage repression thresholds by calculating robustness for 80% and 95% thresholds, and found no qualitative differences. For comparison with the experimental data and the definition of robustness used there, we also calculated robustness as the percentage of all mutants for which >90% of the wild-type repression was retained.

Tunability. Tunability was determined for repressor binding to cognate mutants with repression values between 10% and 90%, as the standard deviation over those mutants for each mutant class. Tunability was calculated for different values of cooperativity (1,3,5,7 kcal mol^{-1}), repressor concentration (1,3,5,7 μM) and RNAP concentration (1,3,5,7 μM). We tested if the results were sensitive to the percentage repression thresholds by calculating tunability for 5% and 20% lower, as well as 80% and 95% upper threshold bound, and found no qualitative differences.

Evolvability. Evolvability was calculated for repressor binding to non-cognate mutants exceeding a threshold of 10% repression. For each mutant class the number of mutants above the threshold was counted and averaged. This procedure was repeated with different values for cooperativity (1,3,5,7 kcal mol^{-1}), repressor concentration (1,3,5,7 μM) and RNAP concentration (1,3,5,7 μM). We tested if the results were sensitive to the percentage repression thresholds by calculating evolvability for 5% and 20% thresholds and found no qualitative differences.

Evolvability on random operators. The promoter region for the random sequence library was based on the *lac* operon[68], because the binding sites for RNAP and repressor do not overlap in this system, thereby avoiding unwanted modifications of RNAP binding by an introduction of a random operator. Binding affinities for

RNAP were calculated for this system using the energy matrix from Kinney et al.[68]. For the operator sites, 1,000,000 random 17bp-long sequences for Lambda CI and 18bp-long sequences for P22 C2 were created in Matlab R2015a. The 1 bp difference in the length of the sites used for the two repressors corresponds to the actual length of their respective cognate operator sites. Binding affinities to these operators were calculated for Lambda and P22 repressors using their energy matrices.

Swapping model parameters of the two repressors and comparing evolutionary properties. We calculated robustness and tunability for Lambda CI after swapping the values for repressor concentration, cooperativity and offset with the respective values for P22 C2. The values were calculated separately for each mutant class (number of mutations). We first swapped each parameter value individually and then we swapped all three parameters with the values of P22 C2. For evolvability, only the values for repressor concentration and offset were swapped individually and simultaneously. The same simulations were done for P22 C2 with Lambda CI parameters. For each evolutionary property, we used a linear regression to determine the R^2 value for the goodness of fit between the reference repressor with its wild-type parameter values and the other repressor with the swapped parameter(s). Regression was carried out across the six mutant classes. The fact that swapping repressor concentrations did not reconcile the evolutionary potential of the two repressors provides further evidence that the experimentally observed differences in the evolutionary potential between the two repressors (Fig. 2) could not be attributed solely to the measured differences in their intracellular concentrations (Supplementary Fig. 1).

Relationship between binding energy and repression. The total binding energy (E_{tot}) is related to gene expression through

$$\text{Gene expression} = \frac{1}{1+[R]e^{E_{tot}-\mu}} \text{ with } E_{tot} = E_{WT} + E_{seq},$$

where μ describes the chemical potential of a repressor. The relationship between binding energy and repression is sigmoidal, with the position of the curve for a given repressor determined by μ and repressor concentration (which we set to 1 for both repressors as we do not want to consider concentration effects here). The same chemical potential and repressor concentration was used for Lambda CI and P22 C2 and taken from Hermsen *et al.*[69]. The positions of a certain operator sequence for a specific repressor on the curve are then given by the total binding energy, E_{tot}, with concentrations for the two repressors being the same. We wanted to develop generic definitions of robustness, tunability and evolvability as properties of only the energy matrix and E_{WT}. The average effect size of one mutation (m) is determined by taking the average of the energy matrix for a given repressor (grand mean over the non-zero entries of the energy matrix, calculated in our example for the six mutated positions) and the deviation in mutational effects (σ) is calculated as standard deviation over all non-zero entries of the energy matrix. Robustness can then be defined as $\text{Rob} = \frac{E_{1/2} - E_{WT}}{m}$ and evolvability as $\text{Evo} = \frac{E_{1/2} - E_{random}}{m}$, where $E_{1/2}$ is the binding energy at half-repression (50%) and E_{random} is the typical binding energy to a random sequence, which will be equal to non-specific binding above a certain number of mutations[42] and is from that point on independent of the energy matrix. Derivation shows that evolvability and robustness are correlated by the number of average mutations between the cognate operator binding energy and the binding energy of a random sequence (#mut), as m determines the positioning of E_{random} relative to E_{WT}: $\text{Evo} = \frac{E_{1/2} - E_{random}}{m} = \frac{E_{1/2} - (E_{WT} + \#\text{mut} \times m)}{m} = \text{Rob} + \#\text{mut}$. This correlation depends critically on two assumptions. First, we assume that the typical mutational effect size (m) is relatively small compared to the offset (E_{WT}) and comparable between different repressors. We base this assumption on the notion that TF–DNA binding is determined by the strength of hydrogen bonds, which range between 1 and 3 kcal mol^{-1} (ref. [47]). The second assumption is that the energy matrix is an intrinsic property of a repressor, meaning that it does not change depending on the DNA sequence that the repressor is binding to. In other words, we assume that m is constant across all binding sites, cognate and non-cognate. Tunability can be defined around $E_{1/2}$ as $\text{Tun} = \left(\sigma \times \frac{d\ \text{repression}}{d\ \text{binding affinity}}\Big|_{E_{1/2}}\right) / \text{Rob}$, where $\frac{d\ \text{repression}}{d\ \text{binding affinity}}\Big|_{E_{1/2}}$ gives the slope of the sigmoid curve at $E_{1/2}$. Positions on the curve for both repressors were calculated for binding to cognate operators, non-cognate operators and the operator with weakest possible binding (according to the energy matrix). Moreover, mean energy values for each mutant class were calculated from model simulations for the cognate and non-cognate operators and placed on the curve. Their locations on the curve provide mean repression values that were then compared to the experimental data through linear regression (Supplementary Fig. 8). Matlab R2015a software was used to calculate the regression, R^2 squared and P values. The fit was similar to the one obtained using the full model (Supplementary Fig. 2).

Lambda cognate O_{R2} mutant library. O_{R2} mutant operators were synthesized analogously to O_{R1} mutants. Based on the assumption that energy matrices between the two closely related operators are likely to be very similar, mutated base pairs in O_{R2} were chosen in positions corresponding to the mutations in O_{R1}. However, the last two were discarded as possibly interfering with RNAP binding (−35 region), leaving four base pairs for mutation (Fig. 2b). Four single, six double, four triple and the quadruple mutant were constructed in the Lambda cognate system and measured as described previously. The fit between data and model was determined through linear regression (Supplementary Fig. 9a).

Lambda cognate O_{R1}–O_{R2} mutant library. O_{R1}–O_{R2} mutant operators were synthesized analogously to O_{R1} mutants, but with one to three mutations in O_{R1} and one to four mutations in O_{R2}. One single, one double and one triple O_{R1} mutant, that showed no decrease in repression, were combined with each of eight randomly selected O_{R2} mutants (two single, three double, two triple and the quadruple). O_{R1}–O_{R2} mutant operators were constructed in the Lambda cognate system, as P22 C2 had very low robustness and hence no trade-off, and measured as described previously. The fit between data and model was determined through linear regression (Supplementary Fig. 9b).

Calculation of epistasis in O_{R1}–O_{R2} mutants. We measured epistasis in two ways. First, we considered its effect on the tunability of the system, where we considered that a given combination of O_{R1}–O_{R2} mutations is in epistasis when the presence of mutations in both operators significantly increased the variance in the observed gene expression levels, compared to the variance achieved by mutations in O_{R1} alone. We compared the variance independently for each mutant class (number of mutations). Second, we calculated epistasis between mutations in the two operators as a deviation from the multiplicative expectation of double mutant repression level based on single mutant effects,

$$\text{epistasis} = \frac{\text{percentage repression}_{O_{R1}-O_{R2}}}{\text{percentage repression}_{O_{R1}} \times \text{percentage repression}_{O_{R2}}},$$

and conducted FDR (false discovery rate)-corrected two-tailed t-tests for each of the double mutants, to determine whether epistasis was significantly different from the null multiplicative expectation (Supplementary Table 6).

Data availability. Experimental data that support the findings of this study have been deposited in IST DataRep and are publicly available at https://doi.org/10.15479/AT:ISTA:108.

Received: 20 February 2018; Accepted: 27 July 2018;
Published online: 10 September 2018

References

1. Jacob, F. & Monod, J. Genetic regulatory mechanisms in the synthesis of proteins. *J. Mol. Biol.* **3**, 318–356 (1961).
2. Englesberg, E., Irr, J., Power, J. & Lee, N. Positive Control of enzyme synthesis by gene C in the L-Arabinose system. *J. Bacteriol.* **90**, 946–957 (1965).
3. Whitacre, J. M. Degeneracy: a link between evolvability, robustness and complexity in biological systems. *Theor. Biol. Med. Model* **7**, 6 (2010).
4. Madan Babu, M., Teichmann, S. A. & Aravind, L. Evolutionary dynamics of prokaryotic transcriptional regulatory networks. *J. Mol. Biol.* **358**, 614–633 (2006).
5. Lozada-Chavez, I. Bacterial regulatory networks are extremely flexible in evolution. *Nucl. Acids Res.* **34**, 3434–3445 (2006).
6. Ciliberti, S., Martin, O. C. & Wagner, A. Innovation and robustness in complex regulatory gene networks. *PNAS* **104**, 13591–13596 (2007).
7. Steinacher, A., Bates, D. G., Akman, O. E. & Soyer, O. S. Nonlinear dynamics in gene regulation promote robustness and evolvability of gene expression levels. *PLoS ONE* **11**, e0153295–21 (2016).
8. Payne, J. L. & Wagner, A. The robustness and evolvability of transcription factor binding sites. *Science* **343**, 875–877 (2014).
9. Tuğrul, M., Paixão, T., Barton, N. H. & Tkačik, G. Dynamics of transcription factor binding site evolution. *PLoS Genet.* **11**, e1005639–28 (2015).
10. Pigliucci, M. Is evolvability evolvable? *Nat. Rev. Genet.* **9**, 75–82 (2008).
11. Isalan, M. et al. Evolvability and hierarchy in rewired bacterial gene networks. *Nature* **452**, 840–845 (2008).
12. Prudhomme, B., Gompel, N. & Carroll, S. B. Emerging principles of regulatory evolution. *PNAS* **104**, 8605–8612 (2007).
13. Ward, J. J. & Thornton, J. M. Evolutionary models for formation of network motifs and modularity in the Saccharomyces Transcription Factor Network. *PLoS Comput. Biol.* **3**, e198–10 (2007).
14. Nocedal, I. & Johnson, A. D. How transcription networks evolve and produce biological novelty. *Cold Spring Harb. Symp. Quant. Biol.* **80**, 265–274 (2016).
15. Tuch, B. B., Li, H. & Johnson, A. D. Evolution of eukaryotic transcription circuits. *Science* **391**, 1797–1799 (2008).
16. Li, H. & Johnson, A. D. Evolution of Transcription networks—lessons from yeasts. *Curr. Biol.* **20**, R746–R753 (2010).

17. Maerkl, S. J. & Quake, S. R. Experimental determination of the evolvability of a transcription factor. *Proc. Natl Acad. Sci., USA* **106**, 18650–18655 (2009).
18. Nocedal, I., Mancera, E. & Johnson, A. D. Gene regulatory network plasticity predates a switch in function of a conserved transcription regulator. *Elife* e23250 (2017). https://doi.org/10.7554/eLife.23250.001
19. Sayou, C. et al. A promiscuous intermediate underlies the evolution of LEAFY DNA binding specificity. *Science* **343**, 645–648 (2014).
20. Pougach, K. et al. Duplication of a promiscuous transcription factor drives the emergence of a new regulatory network. *Nat. Commun.* **5**, 1–11 (2014).
21. Wagner, G. P. & Lynch, V. J. The gene regulatory logic of transcription factor evolution. *Trends Ecol. Evol.* **23**, 377–385 (2008).
22. Hippel von, P. H. & Berg, O. G. On the specificity of DNA-protein interactions. *PNAS* **83**, 1608–1612 (1986).
23. Gerland, U., Moroz, D. J. & Hwa, T. Physical constraints and functional characteristics of transcription factor–DNA interaction. *PNAS* **99**, 12015–12020 (2002).
24. Mustonen, V., Kinney, J. B., Callan, C. G. J. & Lässig, M. Energy-dependent fitness: a quantitative model for the evolution of yeast transcription factor binding sites. *PNAS* **105**, 12376–12381 (2008).
25. Starr, T. N. & Thornton, J. W. Epistasis in protein evolution. *Protein Sci.* **25**, 1204–1218 (2016).
26. Eyre-Walker, A. & Keightley, P. D. The distribution of fitness effects of new mutations. *Nat. Rev. Genet.* **8**, 610–618 (2007).
27. Carroll, S. B. Evolution at two levels: on genes and form. *PLOS Biol.* **3**, e245 (2005).
28. Ludwig, M. Z. et al. Functional evolution of a cis-regulatory module. *PLOS Biol.* **3**, e93–11 (2005).
29. Moses, A. M., Chiang, D. Y., Pollard, D. A., Iyer, V. N. & Eisen, M. B. MONKEY: identifying conserved transcription-factor binding sites in multiple alignments using a binding site-specific evolutionary model. *Genome Biol.* **5**, R98 (2004).
30. Berg, J., Willmann, S. & Lässig, M. Adaptive evolution of transcription factor binding sites. *BMC Evol. Biol.* **4**, 42–12 (2004).
31. Wittkopp, P. J. & Kalay, G. *Cis*-regulatory elements: molecular mechanisms and evolutionary processes underlying divergence. *Nat. Rev. Genet.* **13**, 59–69 (2012).
32. Pujato, M., MacCarthy, T., Fiser, A. & Bergman, A. The underlying molecular and network level mechanisms in the evolution of robustness in gene regulatory networks. *PLoS Comput. Biol.* **9**, e1002865–12 (2013).
33. Sauer, R. T. et al. The Lambda and P22 phage repressors. *J. Biomol. Struct. Dyn.* **1**, 1011–1022 (1983).
34. Ptashne, M. *A Genetic Switch: Gene Control and Phage Lambda.*. (Blackwell Scientific Publications, Palo Alto, CA, US, 1986).
35. Susskind, M. M. & Botstein, D. Molecular genetics of bacteriophage P22. *Microbiol. Rev.* **42**, 385–413 (1978).
36. Sarai, A. & Takeda, Y. Lambda repressor recognizes the approximately 2-fold symmetric half-operator sequences asymmetrically. *PNAS* **86**, 6513–6517 (1989).
37. Hilchey, S. P., Wu, L. & Koudelka, G. B. Recognition of nonconserved bases in the P22 operator by P22 repressor requires specific interactions between repressor and conserved bases. *J. Biol. Chem.* **32**, 19898–19905 (1997).
38. Lutz, R. & Bujard, H. Independent and tight regulation of transcriptional units in *Escherichia coli* via the LacR/O, the TetR/O and AraC/I1-I2 regulatory elements. *Nucl. Acids Res.* **25**, 1203–1210 (1997).
39. Degnan, P. H., Michalowski, C. B., Babić, A. C., Cordes, M. H. J. & Little, J. W. Conservation and diversity in the immunity regions of wild phages with the immunity specificity of phage λ. *Mol. Microbiol.* **64**, 232–244 (2007).
40. Bintu, L. et al. Transcriptional regulation by the numbers: models. *Curr. Opin. Genet. Develop.* **15**, 116–124 (2005).
41. Shea, M. A. & Ackers, G. K. The OR Control system of bacteriophage lambda. A physical-chemical model for gene regulation. *J. Mol. Biol.* **181**, 211–230 (1985).
42. Maerkl, S. J. & Quake, S. R. A systems approach to measuring the binding energy landscapes of transcription factors. *Science* **315**, 233–237 (2007).
43. Zhao, Y., Ruan, S., Pandey, M. & Stormo, G. D. Improved models for transcription factor binding site identification using nonindependent interactions. *Genetics* **191**, 781–790 (2012).
44. Weirauch, M. T. et al. Evaluation of methods for modeling transcription factor sequence specificity. *Nat. Biotechnol.* **31**, 126–134 (2013).
45. Klumpp, S. & Hwa, T. Growth-rate-dependent partitioning of RNA polymerases in bacteria. *PNAS* **105**, 20245–20250 (2008).
46. Razo-Mejia, M. et al. Comparison of the theoretical and real-world evolutionary potential of a genetic circuit. *Phys. Biol.* **11**, 026005 (2014).
47. Lässig, M. From Biophysics to evolutionary genetics: statistical aspects of gene regulation. *BMC Bioinform.* **8**, S7 (2007).
48. Lagator, M., Paixão, T., Barton, N. H., Bollback, J. P. & Guet, C. C. On the mechanistic nature of epistasis in a canonical *cis*-regulatory element. *Elife* e25192 (2017). https://doi.org/10.7554/eLife.25192.001
49. Kreamer, N. N., Phillips, R., Newman, D. K. & Boedicker, J. Q. Predicting the impact of promoter variability on regulatory outputs. *Sci. Rep.* **5**, 18238 (2015).
50. Luscombe, N. M. & Thornton, J. M. Protein–DNA interactions: amino acid conservation and the effects of mutations on binding specificity. *J. Mol. Biol.* **320**, 991–1009 (2002).
51. Watkins, D., Hsiao, C., Woods, K. K., Koudelka, G. B. & Williams, L. D. P22c2 repressor—operator complex: mechanisms of direct and indirect readout. *Biochemistry* **47**, 2325–2338 (2008).
52. Gertz, J., Gerke, J. P. & Cohen, B. A. Epistasis in a quantitative trait captured by a molecular model of transcription factor interactions. *Theor. Popul. Biol.* **77**, 1–5 (2010).
53. Stormo, G. D. & Zhao, Y. Determining the specificity of protein–DNA interactions. *Nat. Rev. Genet.* **11**, 751–760 (2010).
54. Ancel, L. W. & Fontana, W. Plasticity, evolvability, and modularity in RNA. *J. Exp. Zoology Mol. Dev. Evol.* **288**, 242–283 (2000).
55. Draghi, J. A., Parsons, T. L., Wagner, G. P. & Plotkin, J. B. Mutational robustness can facilitate adaptation. *Nature* **463**, 353–355 (2010).
56. Wagner, A. The Role of Robustness in Phenotypic Adaptation and Innovation. *Proc. Roy. Soc. B: Biol. Sci.* **279**, 1249–1258 (2012).
57. Bakk, A. & Metzler, R. *In vivo* non-specific binding of λ CI and Cro repressors is significant. *FEBS Lett.* **563**, 66–68 (2004).
58. Fattah, K. R., Mizutani, S., Fattah, F. J., Matsushiro, A. & Sugino, Y. A comparative study of the immunity region of lambdoid phages including shiga-toxin-converting phages: molecular basis for cross immunity. *Genes Genet. Syst.* **75**, 223–232 (2000).
59. Friedlander, T., Prizak, R., Guet, C., Barton, N. H. & Tkacik, G. Intrinsic limits to gene regulation by global crosstalk. *Nat. Commun.* **7**, 1–12 (2016).
60. Duque, T. et al. Simulations of enhancer evolution provide mechanistic insights into gene regulation. *Mol. Biol. Evol.* **31**, 184–200 (2013).
61. Nagai, T. et al. A variant of yellow fluorescent protein with fast and efficient maturation for cell-biological applications. *Nat. Biotechnol.* **20**, 87–90 (2002).
62. Meyer, B. J., Maurer, R. & Ptashne, M. Gene regulation at the right operator (Or) of bacteriophage II. Or1, Or2, and Or3: their roles in mediating the effects of repressor and cro. *J. Mol. Biol.* **139**, 163–194 (1980).
63. Datsenko, K. A. & Wanner, B. R. One-step inactivation of chromosomal genes in *Escherichia coli* K-12 using PCR products. *PNAS* **97**, 6640–6645 (2000).
64. Koblan, K. S. & Ackers, G. K. Energetics of subunit dimerization in bacteriophage Lambda cI repressor: linkage to protons, temperature, and KCl. *Biochemistry* **30**, 7817–7821 (1991).
65. Santillán, M. & Mackey, M. C. Why the lysogenic state of phage is so stable: a mathematical modeling approach. *Biophys. J.* **86**, 75–84 (2004).
66. Brunner, M. & Bujard, H. Promoter recognition and promoter strength in the *Escherichia coli* system. *EMBO J.* **6**, 3139–3144 (1987).
67. Vilar, J. M. G. Accurate prediction of gene expression by integration of DNA sequence statistics with detailed modeling of transcription regulation. *Biophys. J.* **99**, 2408–2413 (2010).
68. Kinney, J. B., Murugan, A., Callan, C. G. J. & Cox, E. C. Using deep sequencing to characterize the biophysical mechanism of a transcriptional regulatory sequence. *PNAS* **107**, 9158–9163 (2010).
69. Hermsen, R., Tans, S. & Wolde ten, P. R. Transcriptional regulation by competing transcription factor modules. *PLoS Comput. Biol.* **2**, e164 (2006).

Acknowledgements

We thank S. Abedon, R. Grah, K. Jain, C. Nizak, T. Paixão, M. Pleska, E. Reichhart and S. Sarikas for helpful discussions. This work was supported by the People Programme (Marie Curie Actions) of the European Union's Seventh Framework Programme (FP7/2007-2013) under REA grant agreement no. [291734] to M.L., and European Research Council under the Horizon 2020 Framework Programme (FP/2007-2013) / ERC grant agreement no. [648440] to J.P.B. C.I. is the recipient of a DOC (Doctoral Fellowship Programme of the Austrian Academy of Sciences) Fellowship of the Austrian Academy of Sciences.

Author contributions

All authors conceived the study together. C.I. and M.L. designed and carried out the experiments and analysed the data. C.I. wrote the code and ran the model. C.I. and M.L. wrote the initial draft of the manuscript and revised it together with G.T., J.P.B and C.C.G.

Competing interests

The authors declare no competing interests.

Additional information

Supplementary information is available for this paper at https://doi.org/10.1038/s41559-018-0651-y.

Correspondence and requests for materials should be addressed to C.C.G.

nature research

Corresponding author(s): Calin C. Guet

Reporting Summary

Nature Research wishes to improve the reproducibility of the work that we publish. This form provides structure for consistency and transparency in reporting. For further information on Nature Research policies, see Authors & Referees and the Editorial Policy Checklist.

Statistical parameters

When statistical analyses are reported, confirm that the following items are present in the relevant location (e.g. figure legend, table legend, main text, or Methods section).

n/a	Confirmed	
☐	☒	The exact sample size (*n*) for each experimental group/condition, given as a discrete number and unit of measurement
☐	☒	An indication of whether measurements were taken from distinct samples or whether the same sample was measured repeatedly
☐	☒	The statistical test(s) used AND whether they are one- or two-sided *Only common tests should be described solely by name; describe more complex techniques in the Methods section.*
☒	☐	A description of all covariates tested
☐	☒	A description of any assumptions or corrections, such as tests of normality and adjustment for multiple comparisons
☐	☒	A full description of the statistics including central tendency (e.g. means) or other basic estimates (e.g. regression coefficient) AND variation (e.g. standard deviation) or associated estimates of uncertainty (e.g. confidence intervals)
☐	☒	For null hypothesis testing, the test statistic (e.g. *F*, *t*, *r*) with confidence intervals, effect sizes, degrees of freedom and *P* value noted *Give P values as exact values whenever suitable.*
☒	☐	For Bayesian analysis, information on the choice of priors and Markov chain Monte Carlo settings
☒	☐	For hierarchical and complex designs, identification of the appropriate level for tests and full reporting of outcomes
☐	☒	Estimates of effect sizes (e.g. Cohen's *d*, Pearson's *r*), indicating how they were calculated
☐	☒	Clearly defined error bars *State explicitly what error bars represent (e.g. SD, SE, CI)*

Our web collection on statistics for biologists may be useful.

Software and code

Policy information about availability of computer code

Data collection	Matlab R2015a was used for model simulations and to generate random mutant sequences.
Data analysis	R statistical package version 3.3.3. was used for all experimental data analyses.

For manuscripts utilizing custom algorithms or software that are central to the research but not yet described in published literature, software must be made available to editors/reviewers upon request. We strongly encourage code deposition in a community repository (e.g. GitHub). See the Nature Research guidelines for submitting code & software for further information.

Data

Policy information about availability of data

All manuscripts must include a data availability statement. This statement should provide the following information, where applicable:

- Accession codes, unique identifiers, or web links for publicly available datasets
- A list of figures that have associated raw data
- A description of any restrictions on data availability

Experimental data that support the findings of this study (Figures 2 & 6) have been deposited in IST DataRep and are publicly available at https://datarep.app.ist.ac.at/id/eprint/108.

Field-specific reporting

Please select the best fit for your research. If you are not sure, read the appropriate sections before making your selection.

☒ Life sciences ☐ Behavioural & social sciences ☐ Ecological, evolutionary & environmental sciences

For a reference copy of the document with all sections, see nature.com/authors/policies/ReportingSummary-flat.pdf

Life sciences study design

All studies must disclose on these points even when the disclosure is negative.

Sample size	For the overall number of mutants in the experimental section, we conducted a power test that identified we would need 14 different mutants to ensure statistical power of detection (our n=27). These mutants are split into mutant classes based on the number of single point mutations (see Fig.2B and C). The sample size of each mutant class was determined by experimental constraints (for example, we created all six possible single point mutants). See Methods section 'construction of mutant Or1 libraries'.
Data exclusions	no measured data was excluded.
Replication	Adequate replication was determined based on prior experiences working with, and analyzing, similar datasets consisting of population-level plate reader measurements to compare differences in gene expression between mutants.
Randomization	Different mutants and the replicates of each mutant were fully randomized across the required number of 96-well plates (in which the measurements were taken) for each experimental measurement (see Methods section 'Fluorescence assays').
Blinding	Investigators were blinded to group allocation during data collection.

Reporting for specific materials, systems and methods

Materials & experimental systems

n/a	Involved in the study
☒	☐ Unique biological materials
☐	☒ Antibodies
☒	☐ Eukaryotic cell lines
☒	☐ Palaeontology
☒	☐ Animals and other organisms
☒	☐ Human research participants

Methods

n/a	Involved in the study
☒	☐ ChIP-seq
☒	☐ Flow cytometry
☒	☐ MRI-based neuroimaging

Antibodies

Antibodies used	Rabbit 6x-His Tag Polyclonal Antibody (Thermo Fisher, PA1-983B); Rat Anti-HA-Biotin, High Affinity (3F10) (Roche, 12158167001); Goat anti-Rat IgG (H+L) Secondary Antibody, HRP (Thermo Fisher, 31470); Goat anti-Rabbit IgG (H+L) Secondary Antibody, HRP (Thermo Fisher, 31460)
Validation	The manufacturer gives 3 references for the successful use of the rabbit antibodies in Western Blot applications and the rat antibodies were tested by the manufacturer themselves for Western Blot analysis of HA-tagged proteins.